

## Supporting Information

# Interfacial engineering at the 2D/3D heterojunction for high-performance perovskite solar cells

Tianqi Niu,<sup>#,1</sup> Jing Lu,<sup>#,1</sup> Xuguang Jia,<sup>3</sup> Zhuo Xu,<sup>1</sup> Ming-Chun Tang,<sup>4</sup> Dounya Barrit,<sup>4</sup> Ningyi Yuan,<sup>3</sup> Jianning Ding,<sup>3</sup> Xu Zhang,<sup>1,2</sup> Yuanyuan Fan,<sup>1</sup> Tao Luo,<sup>1</sup> Yalan Zhang,<sup>1</sup> Detlef-M. Smilgies,<sup>5</sup> Zhike Liu,<sup>1</sup> Aram Amassian,<sup>4,6</sup> Shengye Jin,<sup>2</sup> Kui Zhao<sup>\*,1</sup> and Shengzhong Liu<sup>1,2</sup>

<sup>1</sup>Key Laboratory of Applied Surface and Colloid Chemistry, Ministry of Education; Shaanxi Key Laboratory for Advanced Energy Devices; Shaanxi Engineering Lab for Advanced Energy Technology, School of Materials Science and Engineering, Shaanxi Normal University, Xi'an 710119, China.

<sup>2</sup>Dalian National Laboratory for Clean Energy; iChEM, Dalian Institute of Chemical Physics, Chinese Academy of Sciences, Dalian, 116023, China.

<sup>3</sup>School of Materials Science and Engineering, Jiangsu Collaborative Innovation Center of Photovoltaic Science and Engineering, Jiangsu Province Cultivation Base for State Key Laboratory of Photovoltaic Science and Technology, Changzhou University, Changzhou 213164, Jiangsu China.

<sup>4</sup>King Abdullah University of Science and Technology (KAUST), KAUST Solar Center (KSC) and Physical Science and Engineering Division (PSE), Thuwal 23955-6900, Saudi Arabia.

<sup>5</sup>Cornell High Energy Synchrotron Source, Cornell University, Ithaca, NY 14850, USA.

<sup>6</sup>Department of Materials Science and Engineering, North Carolina State University, Raleigh, NC, 27695, USA.

KEYWORDS: 2D/3D heterojunction, perovskite solar cell, ligand chemistry, interfacial mechanism, high-performance

\*Corresponding author: E-mail: [zhaok@snnu.edu.cn](mailto:zhaok@snnu.edu.cn)

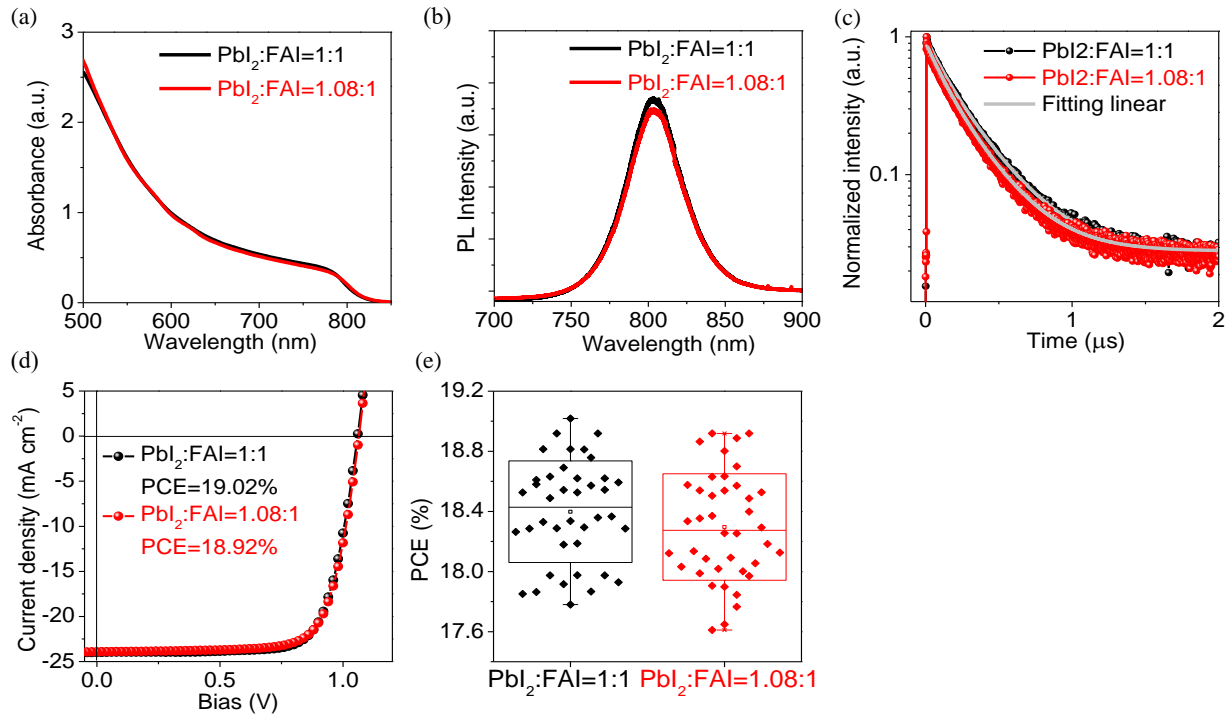


**Figure S1.** (a-c) Steady-state photoluminescence (PL), time-resolved PL spectroscopy (TRPL) and absorption spectra of the FAPbI<sub>3</sub> films with different molar ratio of PbI<sub>2</sub> and FAI. (d) J-V curves of champion devices. (e) Statistics of 40 devices for FAPbI<sub>3</sub> films with different molar ratio of PbI<sub>2</sub> and FAI. Negligible variations in the absorption, emission, carrier lifetime and device performance were observed despite of an extra PbI<sub>2</sub> was introduced, which suggests that the impact of PbI<sub>2</sub> passivation can be excluded.

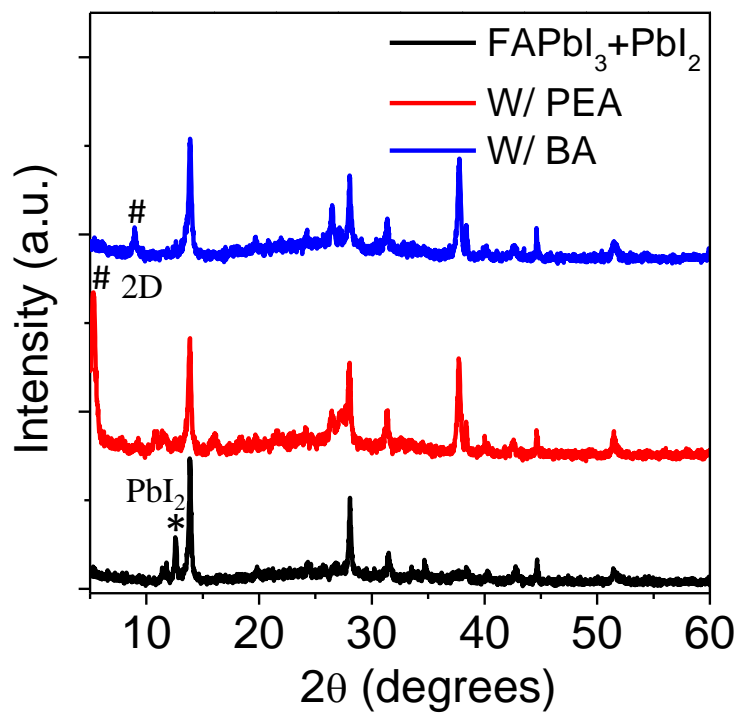


**Figure S2.** X-ray diffraction (XRD) patterns of the FAPbI<sub>3</sub>+PbI<sub>2</sub> and 2D/3D films. Peaks denoted with star and pound signs originate from PbI<sub>2</sub> and 2D perovskite phases.

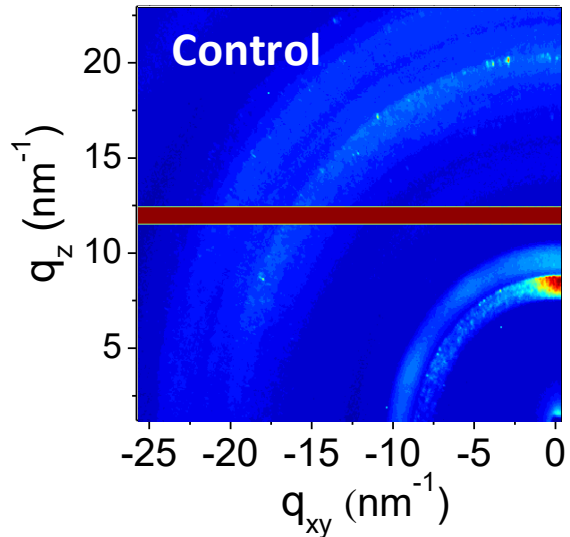


**Figure S3.** *Ex situ* GIWAXS pattern of the control film.

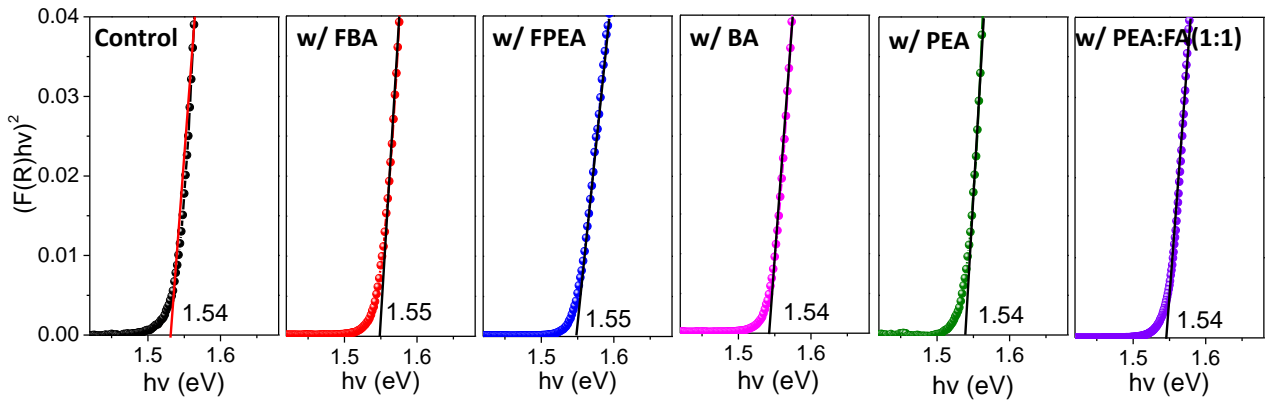


**Figure S4.** Tauc plots for the control, FBA-, FPEA-, BA-, PEA- and PEA:FA(1:1)-based 2D/3D perovskites determining the similar bandgap ( $E_g$ ).

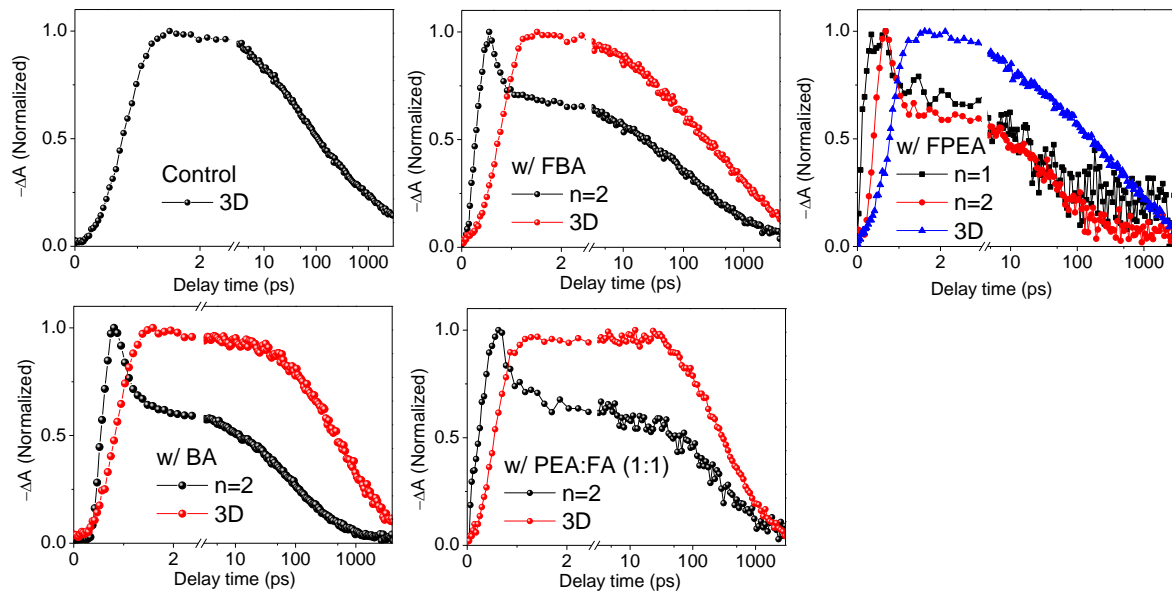


**Figure S5.** The dynamic evolution of the bleaching recovery for the control and 2D/3D films.

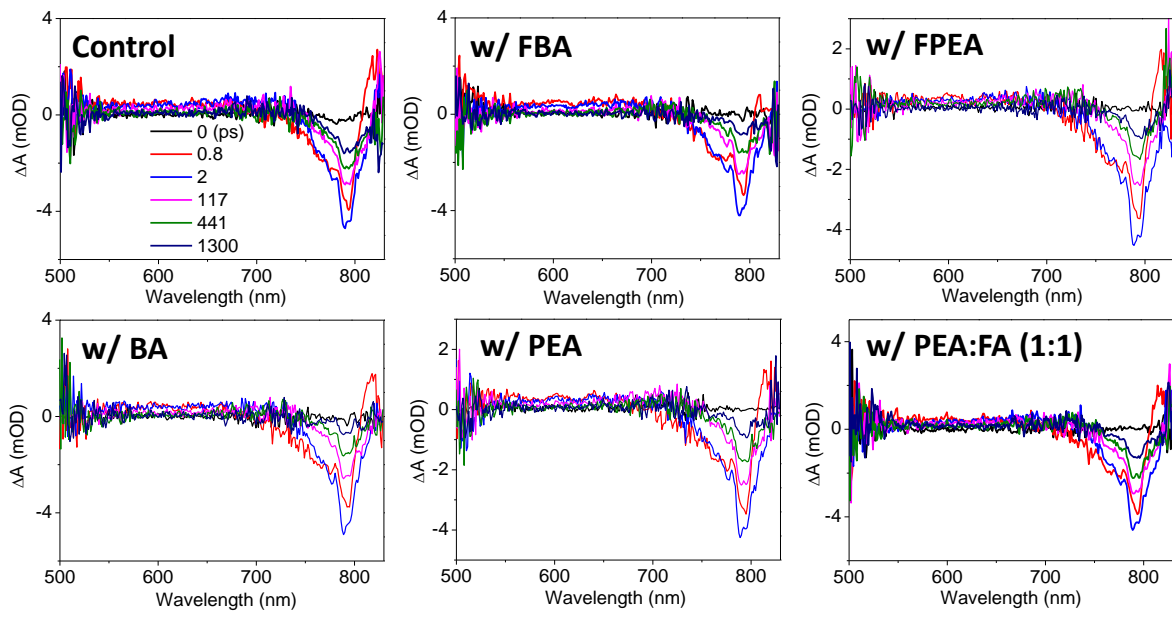


**Figure S6.** Transient absorption (TA) spectra at different delay times of the control and 2D/3D films under back-excitation.

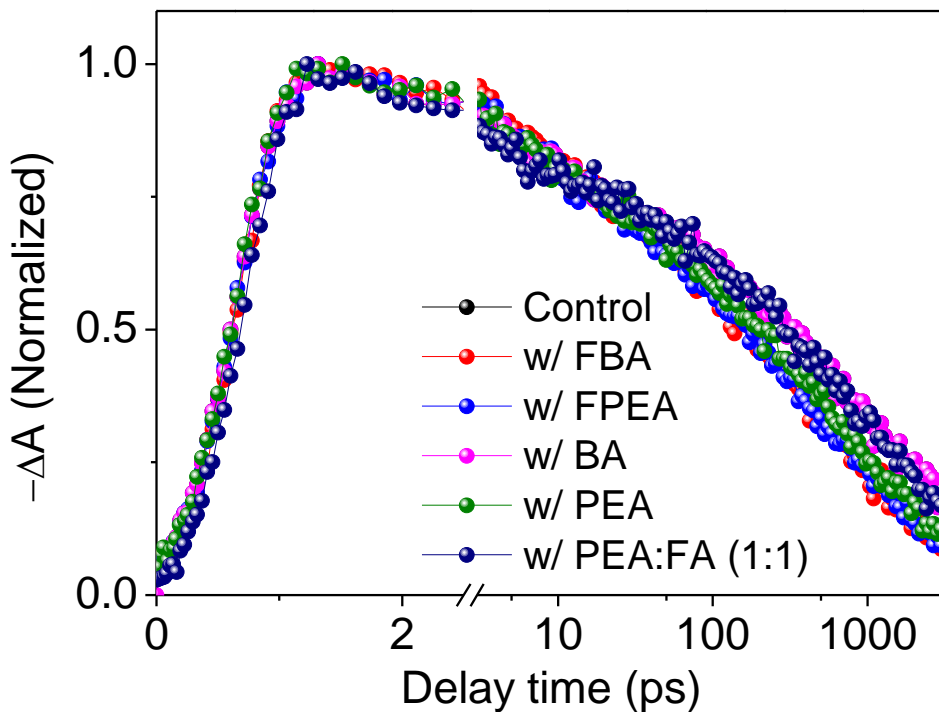


**Figure S7.** TA kinetics of control and 2D/3D films under back-excitation.

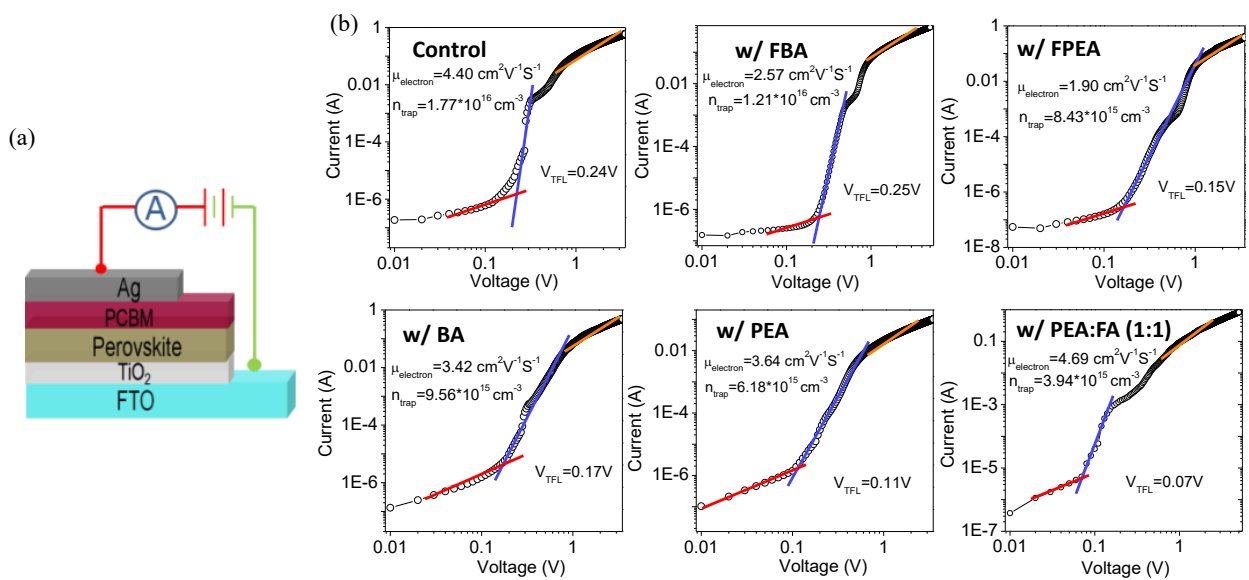


**Figure S8.** (a) The electron-only device structures. (b) Dark  $I$ - $V$  measurement of the electron-only devices for the control and 2D/3D films with different 2D capping layers displaying  $V_{\text{TFL}}$  kink point behavior.

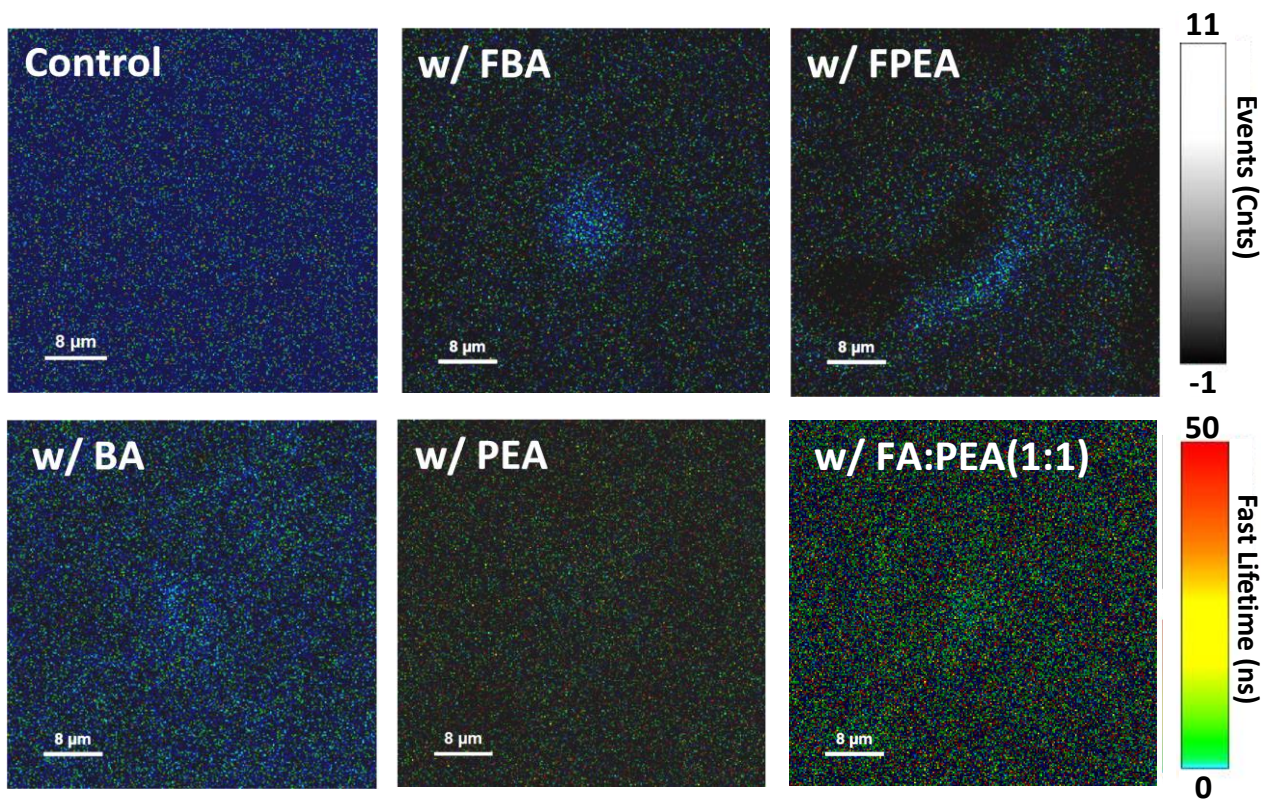


**Figure S9.** Overlapped intensity/lifetime PL mapping images of control and 2D/3D films (the excitation wavelength is 510 nm). The BA-, PEA- and PEA:FA(1:1)-based 2D/3D films exhibit the distinctly increased carrier lifetime accompanied with improved uniformity in contrast to the control film.

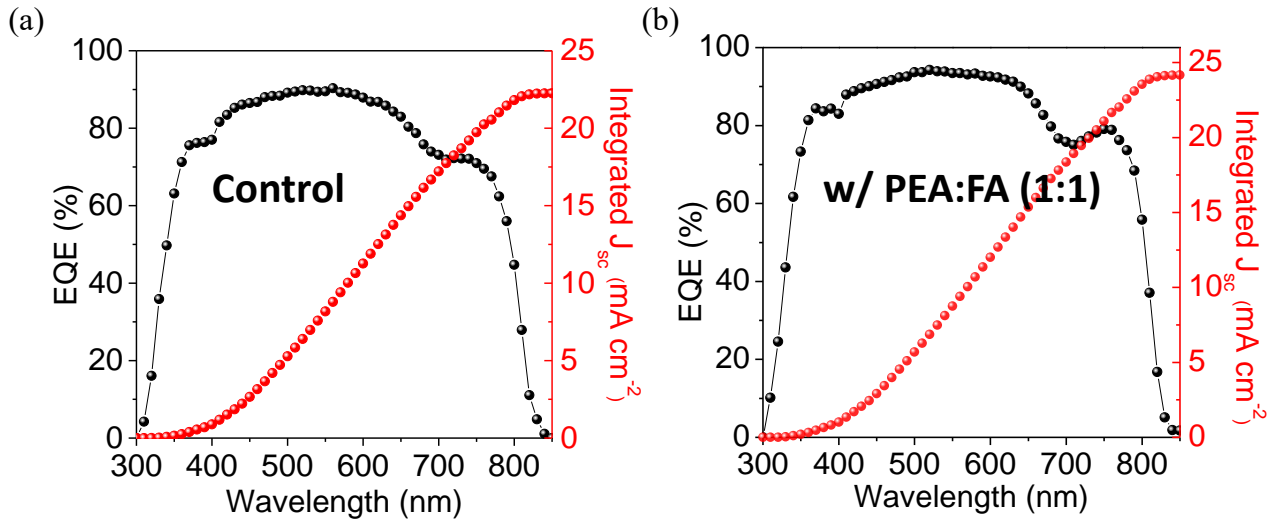


**Figure S10.** (a and b) External quantum efficiency (EQE) and the corresponding integrated short circuit density ( $J_{sc}$ ) for the champion devices obtained for the control and PEA:FA(1:1)-based 2D/3D films.

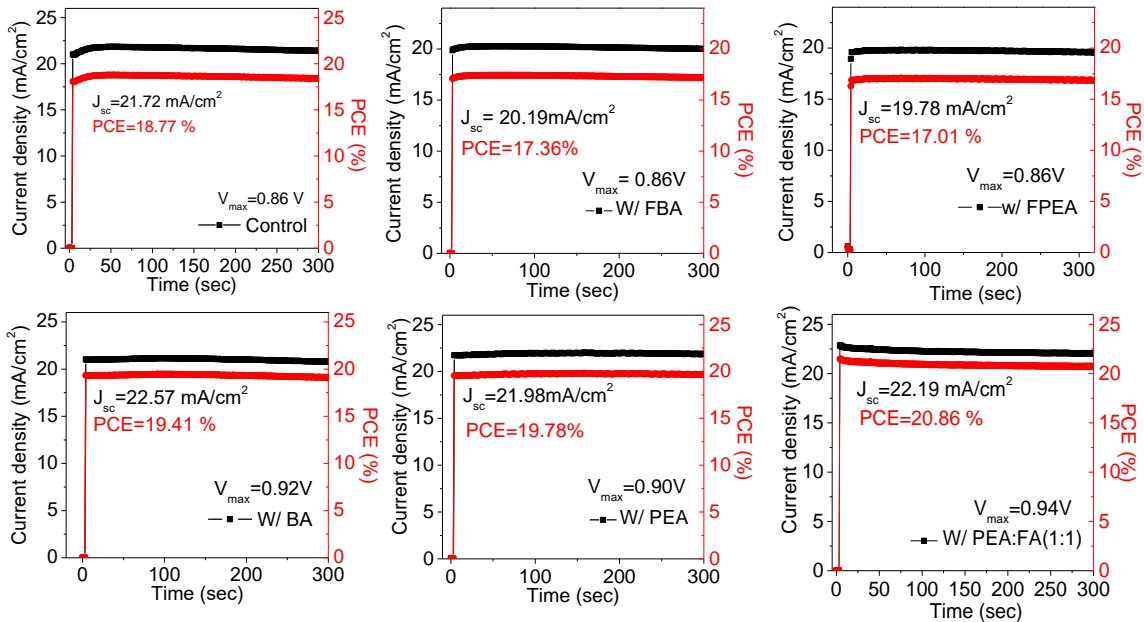


**Figure S11.** The stabilized power output of the champion devices for 2D/3D perovskite measured at a fixed maximum power point (MPP) voltage as a function of time.

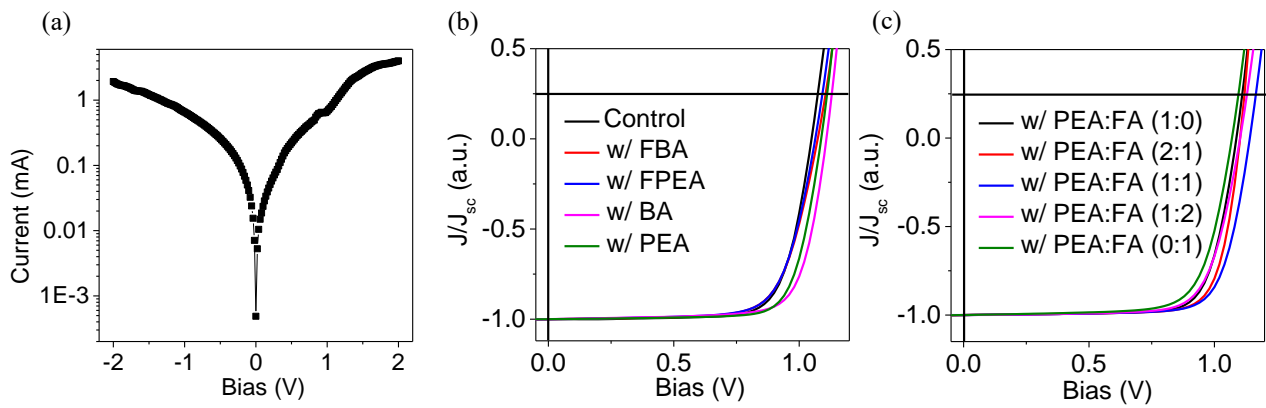


**Figure S12.** (a) The dark J-V curve of the representative control device. The dark curve for the control device is significantly lower than the photocurrent of the same device, suggesting that the contributions from extrinsic resistances are slight to the slopes from  $J$ - $V$  curves at OC and SC. (b) and c) The normalized light  $J$ - $V$  curves of devices for the control and 2D/3D perovskites.

**Table S1.** Photovoltaic parameters of champion devices based on the control and 2D/3D films.

	V <sub>OC</sub> (V)	J <sub>SC</sub> (mA/cm <sup>2</sup> )	FF (%)	PCE (%)
Control	1.06	23.99	74.8	19.02
w/ FBA	1.07	22.63	72.0	17.51
w/ FPEA	1.06	22.13	72.8	17.14
w/ BA	1.11	23.12	76.0	19.50
w/ PEA	1.09	23.76	76.8	19.84
w/ PEA:FA(2:1)	1.10	23.50	78.3	20.28
w/ PEA:FA(1:1)	1.14	24.20	76.6	21.15
w/ PEA:FA(1:2)	1.10	23.69	74.5	19.46
w/ PEA:FA(0:1)	1.07	22.48	73.5	17.68

	V <sub>OC</sub> (V)	J <sub>SC</sub> (mA/cm <sup>2</sup> )	FF (%)	PCE (%)	PCE <sub>max</sub> (%)
Control	1.05±0.01	24.02±0.37	73.1±1.5	18.10±0.46	19.02
w/ FBA	1.05±0.02	22.57±0.31	71.5±2.1	16.95±0.40	17.51
w/ FPEA	1.05±0.01	22.19±0.23	71.8±1.0	16.64±0.65	17.14
w/ BA	1.09±0.02	23.13±0.12	74.7±0.9	18.42±0.42	19.50
w/ PEA	1.08±0.02	23.54±0.35	75.1±1.9	18.86±0.54	19.84
w/ PEA:FA(2:1)	1.07±0.02	23.46±0.32	75.0±1.2	18.71±0.51	20.28
w/ PEA:FA(1:1)	1.10±0.02	23.39±0.56	74.7±1.4	20.21±0.73	21.15
w/ PEA:FA(1:2)	1.06±0.02	23.01±0.42	71.4±1.7	17.47±0.89	19.46
w/ PEA:FA(0:1)	1.05±0.02	22.52±0.48	71.9±0.9	16.99±0.32	17.68

**Table S2.** Summaries of fitting parameters for time-resolved photoluminescence (TRPL) for the different films.

	Control	w/ FBA	w/ FPEA	w/ BA	w/ PEA	w/ PEA:FA(1:1)
A <sub>1</sub>	4446.7	2793.4	6020.6	3429.6	3551.4	7182.2
τ <sub>1</sub> (ns)	211.5	166.8	129.4	301.6	372.1	285.8
A <sub>2</sub>	4857.4	5155.2	4997.4	6496.5	5137.1	2163.3
τ <sub>2</sub> (ns)	50.1	23.3	27.5	57.3	58.9	83.0
τ <sub>ave</sub> (ns)	171.9	137.3	129.4	236.9	313.8	269.5

**Table S3.** The hysteresis parameters of devices based on the control and 2D/3D films.

	Scanning mode	V <sub>OC</sub> (V)	J <sub>SC</sub> (mA/cm <sup>2</sup> )	FF (%)	PCE (%)	Hysteresis index (%)
Control	Reverse	1.06	23.99	74.8	19.02	8.9
	Forward	1.02	23.56	71.8	17.32	
w/ FBA	Reverse	1.07	22.63	72.0	17.51	2.9
	Forward	1.07	22.30	71.3	17.00	
w/ FPEA	Reverse	1.06	22.13	72.8	17.14	5.0
	Forward	1.06	21.60	70.9	16.28	
w/ BA	Reverse	1.11	23.12	76.0	19.50	5.3
	Forward	1.09	22.69	74.9	18.46	
w/ PEA	Reverse	1.09	23.76	76.8	19.84	2.1
	Forward	1.08	23.70	76.0	19.43	
w/ PEA:FA(1:1)	Reverse	1.14	24.20	76.6	21.15	2.9
	Forward	1.13	24.12	75.7	20.54	